Chapter 9

Unfolding veined fold limbs to deduce a basin's prefolding stress state

Koen VAN NOTEN[1,2], Manuel SINTUBIN[2]

[1] Geological Survey of Belgium, Royal Belgian Institute of Natural Sciences, Jennerstraat 13, 1000 Brussels, Belgium

[2] Geodynamics and Geofluids Research Group, Department of Earth and Environmental Sciences, KULeuven, Celestijnenlaan 200E, 3001 Leuven, Belgium

Contact: *koen.vannoten@seismology.be*, *manuel.sintubin@kuleuven.be*

Reference:
Van Noten, K., Sintubin, M., 2019. Chapter 9 - Unfolding Veined Fold Limbs to Deduce a Basin's Prefolding Stress State, in: Billi, A., Fagereng, Å.B.T.-D. in S.G. and T. (Eds.), Problems and Solutions in Structural Geology and Tectonics. Elsevier, pp. 105–116. https://doi.org/10.1016/B978-0-12-814048-2.00009-0

Abstract

Tectonic structures that developed prior to folding, such as pre- and early-kinematic veins, hold valuable information on the stress state of the paleobasin in which these early structures formed. To derive the parental orientation of these prefolding brittle structures, folds need to be 'unfold'. A fold restoration methodology is presented in which fold limbs, and structures they contain, are rotated back to their depositional horizontal position by removing the tilt of the fold hinge line and the dip of individual fold limbs. The method is applied on quartz veins emplaced in folded Lower Devonian sandstones from the High-Ardenne slate belt (Belgium, Germany) and allowed deducing NW-SE opening when the Ardenne-Eifel Basin was at maximum burial depth (early Carboniferous). This exercise can be used in structural geology classes to teach how to rotate data using stereonet techniques hereby encouraging students in applying an unfolding strategy to derive information from prefolding structures.

Keywords

Rotation, Exercise, Folds, Reconstruction, Vein, Extension, Paleostress, Cylindrical folds, Variscan.

9.1 Introduction

The information derived from earlier formed, either sedimentary or tectonic, structures is often 'lost' in orogens because depositional bedding orientation changes during tectonic deformation. The true orientation of primary sedimentary structures such as ripple marks or cross-beds indicate paleocurrent directions during deposition. Hence, restoring bedding to its original depositional orientation prior to deformation can derive these palaeocurrent directions (Lisle and Leyshon, 2004). Other structures such as pre- and early-tectonic fractures and veins, or the attitude of prefolding fault striations, are important markers that hold valuable information on the stress state of the paleobasin prior to the development of folds. Consequently, if a region has been deformed by only one deformation phase, then these primary and pre- and early-tectonic structures can be recovered by a standard rotation exercise in which the beds are restored back to horizontal by 'unfolding' them around the fold hinge line. There are several examples of studies in which the parental orientation of prefolding veins has been investigated using this methodology (e.g. Engelder and Peacock, 2001; Jackson, 1991; Lisle and Leyshon, 2004; Parlangeau et al. 2018; Van Noten et al., 2012). Of crucial importance is the knowledge that the studied features predate the onset of folding. Unfolding around the fold hinge line is rather drastic as the end-member (i.e. the fold) is restored in one time into its original orientation. If the timing of the formation of the studied feature is unclear, more careful restoration techniques should be used in which the geometrical evolution of a fold is restored by unfolding the strata step by step in small steps backward through time (e.g. Vergés et al. 1996). Striae, slickenlines or slickensides related to flexural-slip folding (Tanner, 1989) can for example be studied in this way to investigate when parallelism of striae in opposite fold limbs occurred.

In this chapter, a simple, straightforward fold restoration methodology is presented in which folded beds are restored to their original position prior to folding. Instead of applying the unfolding method on a theoretical and 'perfect' database, we provide a shortened field dataset of extensional quartz veins developed in Lower Devonian sandstone beds (Belgium, Germany) that were folded during the Variscan Orogeny. Because the veins have a prefolding origin, their parental orientation can be used as a palaeostress marker to reveal the paleobasin's stress state during vein emplacement prior to the installation of folds. The database presents orientation data of bedding, cleavage and veins gathered from 16 outcrops in the Variscan High-Ardenne slate belt exposed in Belgium and Germany. Although technological-advanced palinspastic restoration programs do exist, this chapter is constructed such that the rotation exercise can be used in Structural Geology classes to teach how to rotate structures using stereonet techniques. Applying an unfolding restoration exercise manually encourages a geologist (i) to carefully measure and visualise the fold geometry in 3D and (ii) to define a rationale why unfolding needs to be applied. A manual restoration has morever the advantage that one is continuously well aware of the changing orientation of fold limbs, veins and bedding-cleavage intersection because of the different restoration steps. This awareness is less present when using a graphical user – black box – interface restoration program. The results of the exercise can be reproduced either on paper or with a computer stereonet program, e.g. Stereonet (Cardozo and Allmendinger, 2013; used in this chapter) or Open Stereo (Grohmann and Campanha, 2010).

9.2 Regional framework

The dataset is gathered from outcrops exposing low-grade metamorphic rock of the High-Ardenne slate belt (HASB; Belgium, Germany). The HASB forms part of the Variscan Rhenohercynian foreland fold-and-thrust belt in the northern part of the Variscan Orogenic Belt (cf. Oncken et al. 1999). The studied Lower Devonian siliciclastic rocks in the HASB have been deformed during the Variscan Orogeny in the Carboniferous (~ 320 Ma). The veins are mostly contained in (meta)sandstone layers and are at high angle to bedding. Across the HASB, veins are systematically spaced with vein spacing increasing with sandstone thickness (Van Noten and Sintubin, 2010). Veins remain normal to bedding across fold hinges illustrating their prefolding origin. Vein mineralogy (crack-seal structures, fibrous grains, syntaxial growth) shows that fracture opening was normal to the vein walls with quartz minerals being deformed during the later contractional stage (Derez et al., 2016). Mineralogical and fluid inclusion geometry analyses of the vein quartz proved that these veins are extension veins and regionally have an early tectonic origin. Regional vein development occurred when the Lower Devonian Ardenne-Eifel basin was at its maximum burial but at a low differential stress state (Kenis et al. 2002; Van Noten et al. 2011). This particular stress configuration typically occurs when the extensional burial stage comes to an end due to an incipient increasing tectonic stress, heralding a tectonic inversion to the compressional orogenic stage. The low differential stress state is caused by an incipient tectonic stress that increases the magnitude of the horizontal minimum principal stress (σ_3) and which approximates the vertical (burial) maximum principal stress (σ_1) (Van Noten et al. 2012).

The unfolding methodology (see section 9.3) is applied on veins measured in 16 outcrops in six regions. Table 9.1 presents the geographical coordinates of the outcrops. In the northeasternmost part of the HASB (North Eifel, Germany) veins were studied in Pragian outcrops along the shores of the Rursee (R) and Urftsee (U) lakes. In Belgium, veins were measured in Pragian sandstones in an abandoned quarry in Bütgenbach (Bütg.) in the northeastern part of the HASB, in an outcrop in Houffalize (Houff.) and in the Bastogne Mardasson quarry (Bast.) in the central part of the HASB, and in Lochkovian sandstones in a quarry in Bertrix (Bertrix) in the SW part of the HASB (Fig. 9.1).

In the Ardenne-Eifel basin cleavage development was contemporaneous with the single-phase Variscan folding creating a tectonic anisotropy that is consistently axial planar. Because fold hinges are often covered or eroded, fold hingle line measurements are mostly lacking.

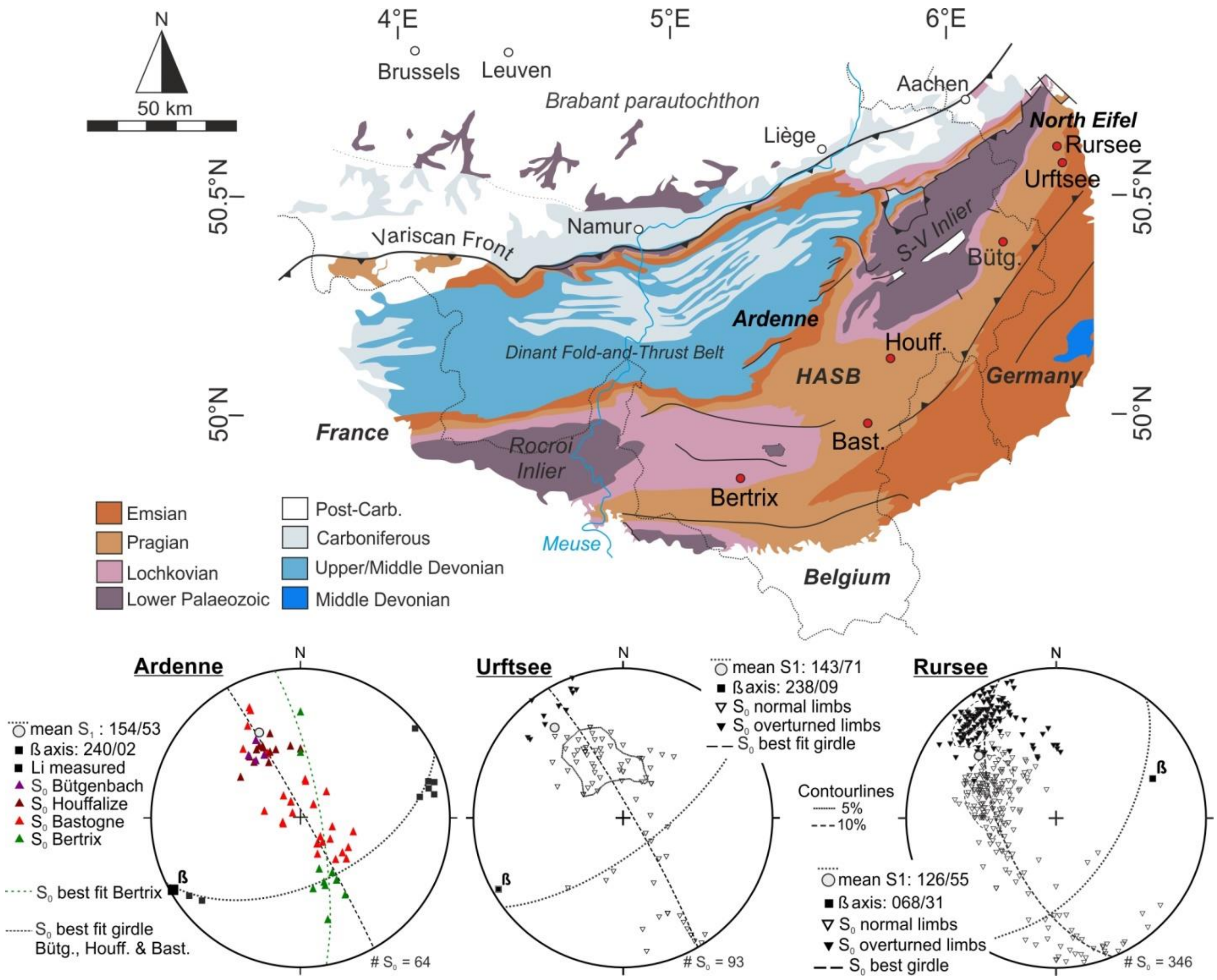

Figure 9.1:a) *Geological setting and structural style of six regions from which vein orientation data has been used. The Rursee and Urftsee study areas are located in the North-Eifel in the NE extremity of the High-Ardenne slate belt (HASB). Bedding poles (S_0) illustrate NW-verging, upright to overturned folds with axial planar cleavage (S_1). 5% and 10% contours illustrate the preferred orientation of normal and overturned bedding poles in the Rursee and Urftsee areas. In the central part of the HASB (Ardenne), folds have an upright and more open attitude and are slightly NWN verging. Towards Bertrix, fold hinges are E-W oriented. Bütg: Bütgenbach; Houff: Houffalize; Bast.: Bastogne.*

9.3 Methodology

To derive the Ardenne-Eifel Basin's stress state during quartz vein emplacement, fold limbs need to be restored back to their inferred horizontal depositional position. Rotations are performed about a horizontal rotation axis in a lower-hemisphere, equal-area Schmidt stereographic projection (stereonet). Rotations follow the rotation procedure as explained in chapter 32 in Lisle and Leyshon (2004): the rotation of a pole (i.e. the normal to a plane) about a horizontal axis follows a cone in space and hence follows a small circle in an equal-area stereonet. For simplification, only the rotational path of bedding is illustrated on Figure 9.3 (see curved grey arrows). For the veins, only orientations measured in the field and restored 'unfolded' orientations are illustrated in this exercise but one should keep in mind that every vein moved along a small circle in the stereonet. When *Stereonet Program* is mentioned in the methodology, it is referred to the Stereonet program of Cardozo and Allmendinger (2013).

Following terminology is used in the methodology and in Figure 9.2:

- *Geometric normal fold limb (nl in Fig 9.2)*: fold limb in which the structural polarity is upwards (sensu Ramsay and Huber, 1987);
- *Geometric overturned fold limb (ol in Fig. 9.2)*: fold limb that has been folded over the vertical; the structural polarity is downwards; to place such a limb in its original horizontal orientation it needs to be unfolded over the vertical for more than 90°;
- *Fold hinge line (FHL)*: measured line of maximum curvature within a folded surface*;*
- *Bedding-cleavage intersection lineation (Li)*: assuming cylindrical folding with an axial planar cleavage, Li can be used as a proxy of the FHL in deformed areas with a single deformation phase; under these conditions the FHL-parallel Li is also defined as the fold axis;
- *Rotation axis (RA)*: an imaginary axis over which a fold or a fold limb will be rotated; in nature, this axis does not always have a physical expression (e.g., axis normal to the FHL);
- *Angle of rotation (Ar in Fig. 9.2)*: value over which a FHL or a fold limb needs to be rotated;
- *β-axis:* pole to the best-fit plane (dashed line in stereoplots in Fig. 9.1) through all bedding poles; parallel to the FHL of cylindrical folds; derived from stereoplot analysis (see bedding plots in Fig. 9.1).

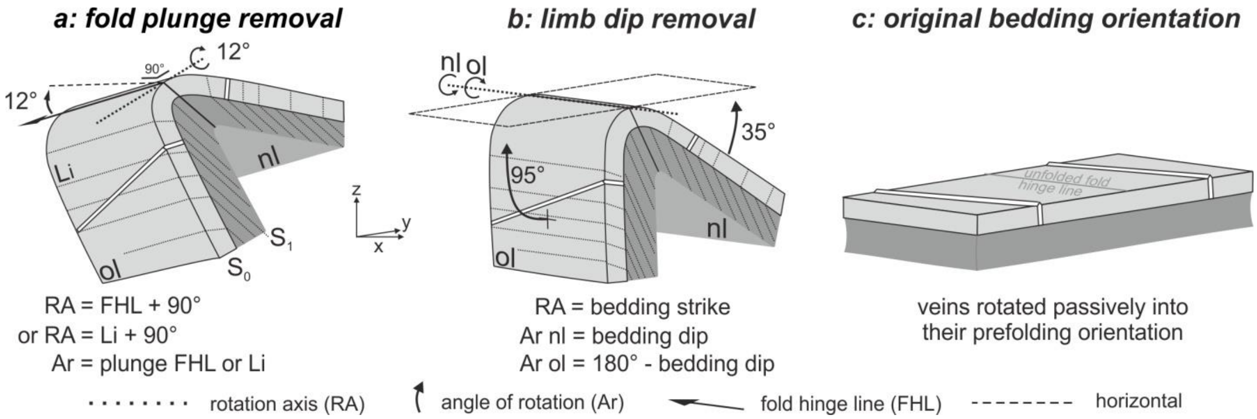

Figure 9.2: *Unfolding a fold: two necessary steps to restore the beds to their original prefolding horizontal orientation.* ***a: fold plunge removal:*** *removing the plunge of the fold by rotation around a horizontal axis (RA) oriented normal to either the FHL or the Li with the plunge of the FHL or Li as angle of rotation (Ar).* ***(b) limb dip removal:*** *unfolding the fold limbs to horizontal around the untilted FHL or around the strike of the untilted bedding with the bedding dip as rotation angle for normal limbs (nl) and 180° - bedding dip as rotation angle for overturned limbs (ol). Stereonet Program convention is used in which a clockwise rotation is positive and an anticlockwise rotation is negative when looking down along the plunge of the FHL.* ***(c)*** *Reconstructed presumed* ***original bedding orientation*** *with veins rotated passively to their original prefolding orientation. The rotation values are illustrative examples. S_0: bedding; S_1: cleavage; Incompetent unit: dark grey; competent unit: light grey.*

In what follows the unfolding rotation exercise is carefully explained in different steps:

1. First, all available planar data, i.e. bedding, cleavage and veins, need to be plotted as **poles** in a stereonet. Using the pole instead of a great circle is convenient because poles facilitate the understanding of the different steps during the rotation.
2. Use bedding and cleavage orientation data for each outcrop to calculate the orientation of **Li** to decipher the plunge of the local FHL. For each outcrop or sandstone bed for which the unfolding exercise is applied, you take the average of the intersection lineations as the representative of the local FHL.
3. **Remove the local plunge of each fold** by rotating the complete dataset, i.e. the fold limb with the veins it contains, about a virtual horizontal rotation axis (RA in Table 9.1) oriented normal to the FHL or the Li (dotted line on Fig. 9.2a). To remove the plunge of the FHL the dataset needs to be rotated using a rotation axis with orientation *FHL (or Li) + 90°* and with the *plunge of the FHL* (or Li when the FHL is not materialised) as angle of rotation. Beware to rotate in the proper direction over an angle smaller than 90°. As result of the fold plunge removal, the orientation of the fold limbs (and the veins) will be slightly changed and the bedding strike will be similar to the trend of the untilted fold hinge line.
4. The next step consists of **restoring each individual fold limb to its original horizontal orientation** (Fig. 9.2b). To evaluate if similar vein generations are present in different fold limbs, each fold limb needs to be restored separately by using the strike of the rotated bedding (which is parallel to the untilted local FHL or Li) as rotation axis. For geometric normal fold limbs, the

bedding dip needs to be used as value of rotation. Overturned fold limbs need to be rotated over the vertical for a value of *180° - bedding dip* (Fig. 9.2). In a 3D world this rotation occurs in a vertical surface defined by the newly acquired (after step 3) dip direction and the normal to the trend of the untilted FHL and the untilted bedding strike. The *Stereonet Program* convention is used in which a clockwise rotation is positive and an anticlockwise rotation is negative when looking down along the plunge of the FHL (see Table 9.1). Unfolding both limbs results in a coplanar horizontal bedding.

5. Once the beds are restored to their presumed original horizontal orientation (Fig. 9.2c), veins of different limbs can be merged in a single stereonet to compare the original orientation in the geometric normal and overturned fold limbs for similarity.

One has to keep in mind that the unfolding methodology described in this chapter only works for single-phase deformed orogens in which hardly any orogenic rotation has occurred. It is thus advised to first gather regional information on the studied orogen and its deformation phase(s) before applying this methology.

9.4 Results

For each region in which the rotation exercise is applied, the structural architecture is briefly introduced to frame the measurements. The location of the discussed outcrops and the orientation data of bedding, cleavage, bedding-cleavage intersection lineation are presented in Table 9.1. To visualise bedding and cleavage structural data in Google Earth™ one can generate a kml of the data using e.g. the open source GeoloKit program (Triantafyllou et al. 2017). The observed orientation of veins is presented in Tables 9.2 and 9.3. If this exercise is used in structural geology classes, the *measured data* columns can be provided as source whereas the *derived data* columns need to be calculated from bedding and cleavage data in a stereonet using the methodology described in section 9.3. The results of the unfolding exercise of each outcrop is shown in Figure 9.3.

9.4.1 Rursee, North Eifel, Germany

The Rursee lake is located 30 km ESE of Aachen (Germany). Lower Devonian (upper Pragian) alternating slaty and coarse-grained sandstone sequences present along the shores of the lake are continuously exposed in autumn when the lake waterlevel is low. These sequences are folded in second order, NW-verging, upright to overturned folds with subangular and subrounded fold hinges and moderately SE-dipping axial surfaces. Bedding changes from gently SE-dipping to either steeply NW-dipping in the upright folds, or to steeply SE-dipping with an overturned structural polarity in overturned folds. Bedding poles of the overturned folds are dominantly present in two clusters on the Rursee stereonet (Fig. 9.1) which is representative of subangular tight folds. Bedding poles of the upright folds show a scattered distribution along a mean girdle which is representative of cylindrical folds (Twiss and Moores, 1992). The gently NE-plunging mean bedding-cleavage intersection lineation is parallel to the β-axis of the best fit through the bedding poles illustrating the parallellity of cleavage with the axial surfaces. The NW-verging attitude of both fold styles corroborates the Variscan deformation style in the North Eifel. This typical deformation style is caused by compression of the Lower Devonian deposits against the rigid Lower Palaeozoic Stavelot-Venn Massif NW of the North Eifel (Fig. 9.1). The variability in fold style is represented by seven selected outcrops. Overturned fold limbs are shown in R1, R5 and R6, SE-dipping normal limbs in R3 and R4, and NW-dipping normal limbs in R2 and R7 (Fig. 9.3). To unfold these fold limbs, the largest rotation needs to applied for the overturned fold limbs.

Table 9.1: *Location and orientation data of 16 outcrops in the HASB. RA: Rotation axis. The convention of the Stereonet Program (Cardozo and Allmendinger, 2013) is used in which a clockwise rotation is positive and an anticlockwise rotation is negative when looking down along the FHL. Vein orientation data are provided in Table 2. *Only in Bertrix the FHL could be measured and can be used as rotation axis. Data sources: Kenis (2004) and Van Noten (2011). Convention used: dip direction (dd) / dip (d). Bütg.: Bütgenbach; Houff.: Houffalize; Bast.: Bastogne.*

		Measured data								Derived data					
	Outcrop	Limb dip	location		S_0		S_1		Li		untilt RA		unfold RA	
			lon	lat	dd	d	dd	d	dd	d	dd	d	dd	d
Rursee	R1	SE (ol)	6.399888	50.633868	143	86	126	60	55	30	145	30	55.3	94.5
	R2	N	6.400745	50.633078	335	38	132	45	52	10	142	10	52	36.9
	R3	SE	6.401802	50.632414	120	41	131	50	67	28	157	28	67.6	-31.6
	R4	SE	6.401267	50.632359	111	42	122	60	43	19	133	19	43.5	-38.3
	R5	SE (ol)	6.402633	50.631278	146	75	138	50	59	13	149	13	59.5	105.3
	R6	SE (ol)	6.402999	50.630882	140	74	134	51	53	11	143	11	52.2	106.3
	R7	N	6.412318	50.642765	340	80	120	35	66	22	156	20	75.6	81.2
Urftsee	U1	SE	6.461016	50.583945	170	48	165	58	245	15	335	15	66	-45.9
	U2	NW	6.461546	50.583623	282	25	130	70	216	11	306	11	36.6	22.7
	U3	SE	6.461546	50.583623	196	30	141	70	220	27	310	27	43.9	-11.8
	U4	SE	6.461733	50.583488	212	17	130	74	215	18	305	18	165.6	1.3
	U5	SE	6.461733	50.583488	158	40	154	61	240	7	330	7	59.6	-39.5
Ardenne	Bütg.	SE	6.256375	50.420963	140	45	142	64	53	3	143	3	53	-44.9
	Houff.	SE	5.789722	50.128889	150	40	155	65	69	8	159	8	70.1	-44.6
	Bast.	NW	5.739167	50.013889	318	18	152	62	240	5	330	5	63.6	17.6
	Bertrix	NW	5.22745	49.875258	340	40	160	55	75*	8*	165	8	87.8	-46.2

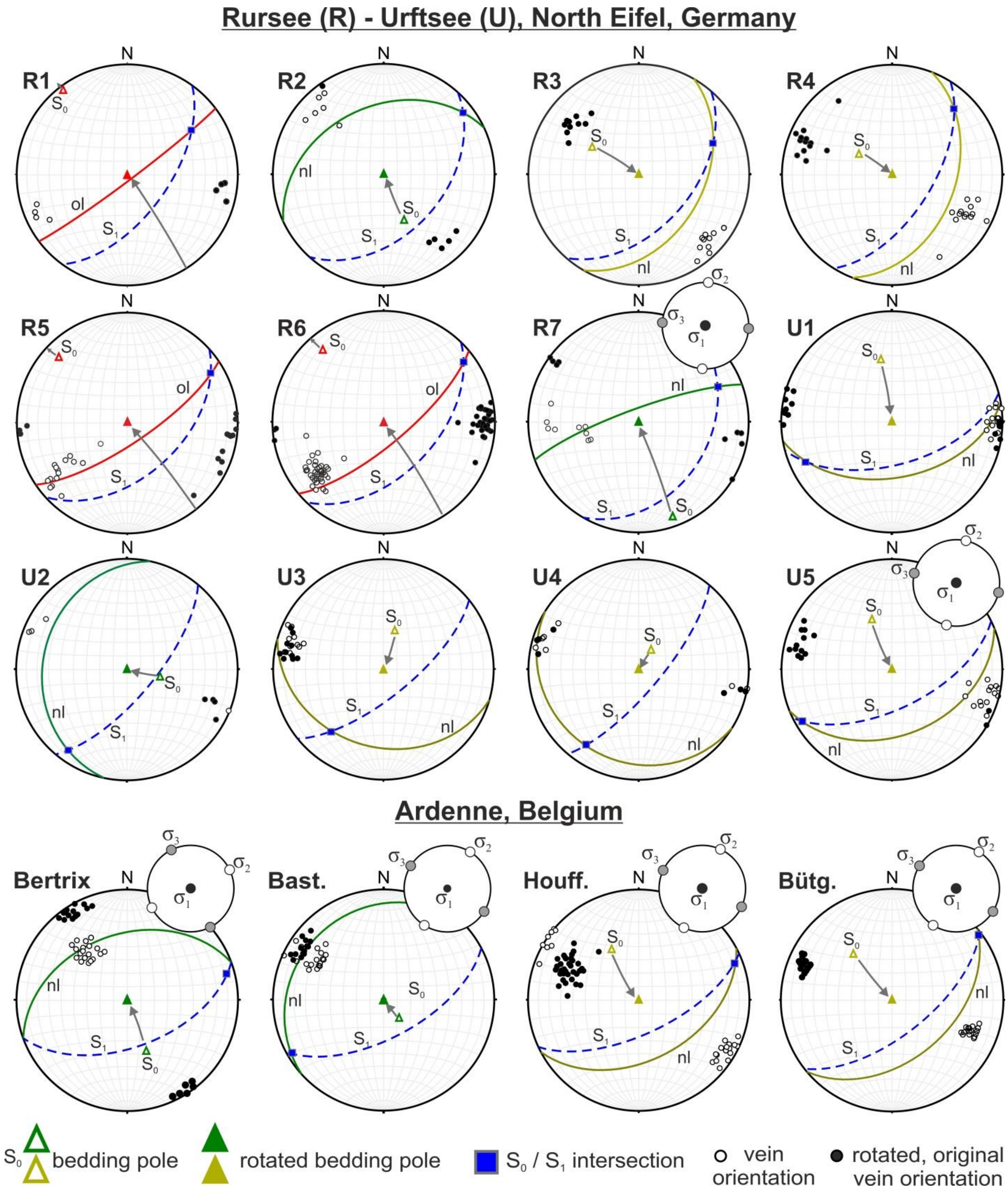

Figure 9.3: *Unfolding methodology applied to 16 vein datasets. In each lower-hemisphere, equal-area stereographic projection a sandstone bed is, together with the veins it contains, unfolded to horizontal. The unfolding trajectory of bedding along a small circle is illustrated by a grey arrow. Overturned SE-dipping limb (ol): red; normal NW-dipping limb (nl): green; normal SE-dipping limbs (nl): yellow. S_0: bedding; S_1: cleavage. The small insets indicate minimum (σ_3), intermediate (σ_2) and maximum (σ_1) principal stresses after a paleostress analysis on the unfolded veins. Insets in R7 and U5 show the paleostress results of all unfolded veins of the Rursee and Urftsee, respectively. For color version of this figure, the reader is referred to the online version of this book.*

Table 9.2: *Vein orientation data of 12 outcrops in the North Eifel (Germany). Convention used: dip direction (dd) / dip (d).*

R1		R2		R3		R4		R5		R6				R7		U1		U2		U3		U4		U5	
dd	d	dd	d	dd	d	dd	d	dd	d	dd	d	dd	d	dd	d	dd	d	dd	d	dd	d	dd	d	dd	d
72	75	138	70	316	80	298	60	52	25	225	30	232	30	90	72	190	80	122	75	105	68	280	75	280	80
65	80	132	72	318	85	298	65	60	65	234	20	228	30	86	71	180	75	111	84	106	70	280	90	276	76
68	79	125	75	308	75	305	60	60	50	228	15	232	25	85	65	182	80	112	82	104	76	109	80	294	70
60	70	140	80	315	72	302	54	56	65	235	30	220	20	102	70	178	85	292	89	110	75	102	85	280	60
75	30	144	80	312	70	288	61	54	50	225	15	232	35	70	38	172	78			108	79	108	81	290	60
59	20	138	50	302	80	292	66	59	55	228	20	230	28	85	45	178	80			115	81	102	75	310	82
75	25			302	80	300	65	50	80	226	24	228	25	78	40	185	75			100	80	120	73	279	85
85	28			326	84	298	70	54	66	242	25	240	30	85	40	170	85			108	65			280	88
162	85			312	75	296	85	54	75	238	28	234	25	70	40	172	84			115	85			283	85
				320	75	296	70	58	65	240	20	230	30			173	90			100	75			284	89
				315	70	300	60	42	78	245	35	230	20			180	85							128	80
				262	79	286	70	50	78	260	30	235	32			178	86							116	78
						330	75	52	70	245	30	232	20			180	85							110	82
						111	42	48	45	228	50	235	28			178	86							118	79
								54	78	230	35	232	29			186	86								
								50	80	230	25	238	19			180	89								
										230	22	238	20												
										222	20														

Bedding-normal veins exist in all fold limbs and veins vary in thickness. Millimeter-thick hairline stratabound veins, milky-white, centimeter-thick veins with several phases of crack-seal quartz infill, and composite centimeter-thick veins composed of several quartz laminae separated by host-rock inclusion fragments oriented parallel to vein wall all occur (Fig. 9.4, R6; Van Noten et al. 2008, 2009). Unfolding the overturned and NW-dipping normal limbs results in veins dipping steeply to subvertical to the ESE and SE. Unfolding SE-dipping normal limbs results in a NW-dipping original vein orientation.

9.4.2 Urftsee, North Eifel, Germany

The Urftsee lake is located in the North Eifel, 5 km SSE of the Rursee lake. Upper Pragian to Lower Emsian sandstone, siltstone and slaty sequences are deformed in cylindrical folds with associated moderately to steeply SE-dipping axial planar cleavage. β-axis of the best fit through the bedding poles is subhorizontal (Fig. 9.1). Fold hinges vary from gently SE-dipping to gently NW-dipping giving rise to slightly NW-verging, upright folds. This fold style slightly differs from the fold style observed in the Rursee area as overturned folds are barely present in the Urftsee area. The outcrops studied are situated on a higher structural level than those of the Rursee outcrops.

Bedding-normal quartz veins are ubiquitous present and have similar characteristics as those of the Rursee. They remain orthogonal to bedding around fold hinges and refract at the competent-incompetent interface. Veins are straight or lensoid in shape and have a fibrous infill. Veins can be traced along several meters on bedding planes. These observations allow attributing a prefolding and pre-cleavage origin to the veins. Four gently SE-dipping normal limbs (U1, U3-U5) and one gently NW-dipping limb (U2) are selected to be unfold (U1 to U5 in Tables 9.1 and 9.2 and in Fig. 9.3). These outcrops belong to an open fold train in which intervein distance is commonly equally spaced (Fig. 9.4, U3). Because fold hinges are subhorizontal and bedding dip is gentle, the original veins orientation after unfolding does not differ that much from the vein orientation in the folded limbs. After unfolding veins trend NNE-SSW (Fig. 9.3).

9.4.3 Intermullion veins, High-Ardenne slate belt, Belgium

Bedding-normal veins can be found in Lower Devonian sandstones in the entire southern part of the HASB. Deformation is characterised by a NW-SE structural grain materialised by slightly NW- to N-verging open cylindrical folds, with SE- to S-dipping slaty cleavage (Asselberghs, 1946). Four outcrops are selected to compare original vein orientations of the northeastern and central parts of the HASB. Contrary to the described outcrops in the North Eifel, outcrops in the Ardenne show the presence of mullion structures, i.e. cylindrical cuspate-lobate structures at the sandstone-pelite compentent-incompent interface, formed by initial layer-parallel Variscan shortening after bedding-normal veining (Kenis et al. 2002, Kenis 2004). Throughout the HASB, spacing of the bedding-normal veins is related to the thickness of the individual competent banks in which they developed (Van Noten and Sintubin, 2010).

Bütgenbach

Vein measurements come from an abandoned quarry east of the Bütgenbach lake where Pragian sandstones alternate with dark silty pelites. The outcrop is located in a gently, SE-dipping limb with normal structural polarity belonging to a second-order syncline. Bedding-cleavage intersection is subhorizontal reflecting an upright position of regional folds. Veins occur in layers of different thickness but mostly veins are non-stratabound: i.e. continuing through the sandstone-pelite interface. Vein filling is granular blocky of dominantly quartz. Unfolding results in steeply NW-dipping veins with a dip opposite to the veins before unfolding.

Houffalize

The selected outcrop in Houffalize is located in a moderately, SE-dipping normal limb of a first-order folded syncline. Veins are developed in grey psammites emplaced in dark pelites. Tectonic cleavage is steeply SE-dipping (Table 9.1) and axial planar to the slightly NNW-verging upright folds. Both blocky and fibrous vein infill is observed. Mullion structures are not pronounced in thin psammites beds (Fig.

9.4). Unfolding results in NW-dipping veins which are slightly obliquely oriented to bedding when restored to their original orientation.

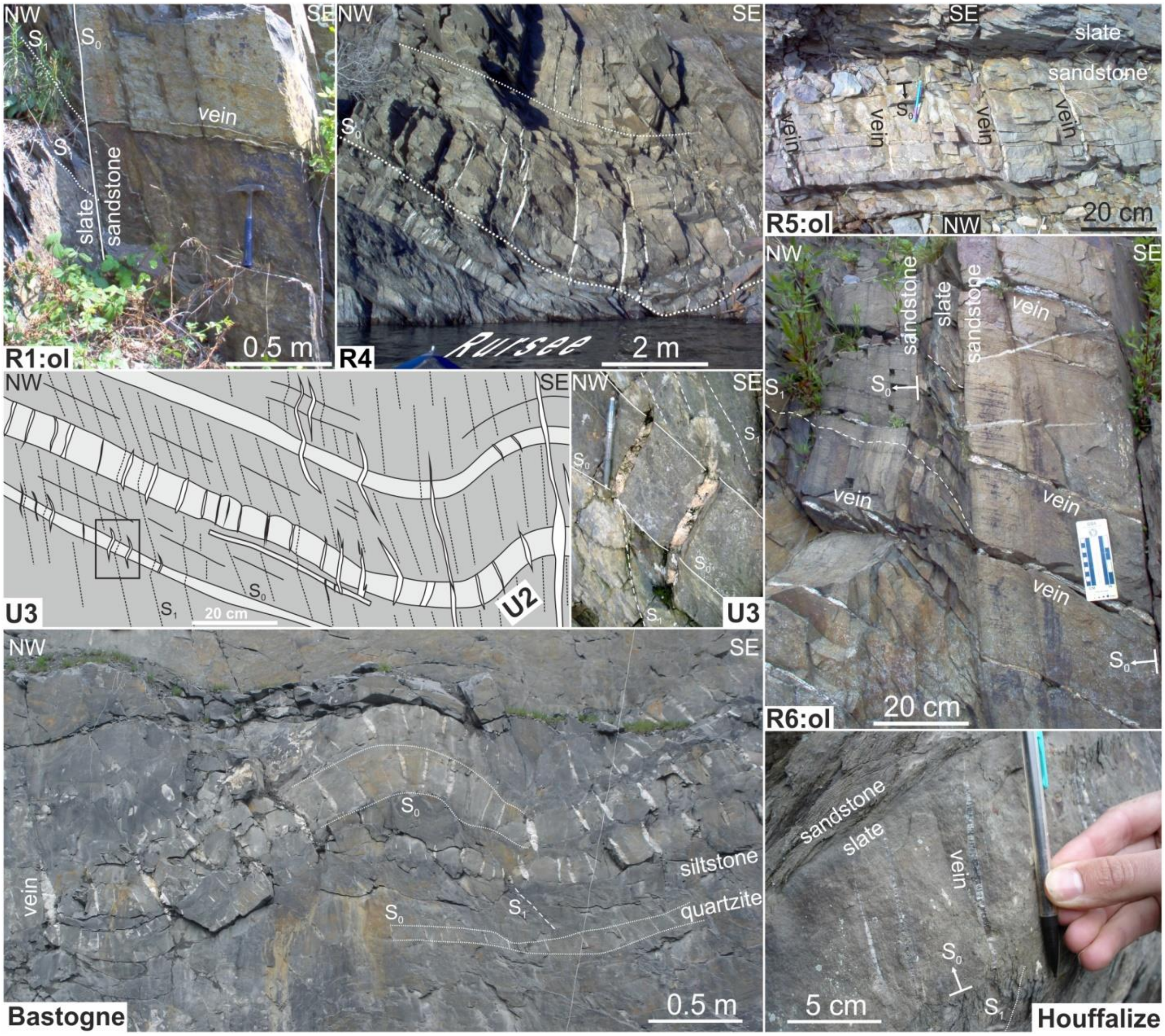

Figure 9.4: *Examples of bedding-normal veins in sandstones and quartzites from selected outcrops along the Rursee (R) and Urftsee (U) lakes in the North Eifel and from the Bastogne Mardasson quarry and the Houffalize outcrop in the Ardenne. Veins remain at high angle to bedding no matter the orientation of the hosting competent bed. ol: overturned limb;* S_0*: bedding;* S_1*: cleavage.*

Table 9.3: *Vein orientation data of 4 outcrops in the Ardenne (Belgium). Convention used: dip direction (dd) / dip (d). Bast.: Bastogne.*

Bast.		Houffalize				Bütgenbach				Bertrix			
dd	**d**	**dd**	**d**	**dd**	**d**	**dd**	**d**	**dd**	**d**	**dd**	**d**	**dd**	**d**
128	65	110	85	298	82	292	70	291	65	40	45	48	50
128	56	120	90	298	79	295	58	294	60	40	50	50	60
124	55	120	85	300	85	295	70	288	65	44	40	50	45
134	62	122	82	300	80	296	60	288	70	45	60	50	40
127	60	125	90	300	75	294	70	290	70	45	55	50	52
124	85	128	90	304	87	294	65	290	60	45	60	50	45
114	75	130	90	305	82	292	64	285	70	45	45	55	50
112	62	130	88	305	75	290	63	145	60	45	50	55	55
118	55	290	85	305	74	290	70	142	64	47	40	60	40
120	56	295	88	308	78	288	70	145	65	48	40	60	55
121	60	295	85	310	85	290	62			65	40	60	45
124	56	295	75	310	76								
115	56	296	80										
118	56												
115	66												
116	62												

Bastogne Mardasson

The quarry of Mardasson in Bastogne is famous as the term 'boudin' and 'boudinage' originally have been used for the first time (Lohest et al., 1908) for the cuspate-lobate structures that now are renamed into mullions (Kenis and Sintubin 2007). In the quarry, alternating blue siltstones and blue quartzites are excavated. Veins are developed in the competent quartzites layers that have a complex sedimentology (Fig. 9.4). The quarry outcrops a hectometric open, upright, slightly NW-verging anticline. Quartzites are all fractured by symmetric lensoid veins that are mostly limited to the competent layers. Due to their restriction to the competent layers and the complex sedimentology, veins vary in length and width. Veins are thicker if they are enclosed in multilayers. The vein measurements (Table 9.3) come from a gentle NW-dipping limb of the anticline. Because of the gentle bedding dip of the outcrop and the minor rotation applied, unfolding results in only a slight change of the vein orientation into steeply to upright NW-dipping veins.

Bertrix

The quarry of Bertrix in the SW part of the HASB excavates blue quartzites alternating with blue dark pelitic siltstones of Lochkovian age. In individual beds where lensoid veins are present, veins are generally limited to the quartzitic layers. The measurements were made on the NW-dipping normal limb of a second-order upright anticline. After unfolding, veins are subvertical with steep dips to the NW and SE. This original orientation slightly deviates from the restored veins from the Bütgenbach, Houffalize and Bastogne outcrops.

9.5 Discussion

9.5.1 Opposite dip of unfolded veins

After unfolding, most veins of the North Eifel are not perfectly perpendicular to bedding but are rather at ~ 80° to bedding. This implies that either veining did not develop perpendicular to bedding and hence that beds were already tilted at the time of veining or that veins were initially perpendicular to bedding but afterwards were deformed into their sub-perpendicular attitude. Arguments in favor for the latter mechanism are the curved veins in overturned limbs (R6 in Fig 9.4) and opposite dip of veins from normal limbs versus veins from overturned limbs after unfolding. After unfolding, veins in normal limbs (R3, R4, U3, U4, and U5) dip to the ESE whereas veins in overturned limbs (R1, R5, R6) and NW-dipping normal limbs (R2, U2) dip to the WNW (Fig. 9.3). This opposite vein orientation is in agreement with the change in orientation that is expected from flexural flow during folding (Tanner, 1989).

Veins in sandstones in overturned limbs often show a curved nature whereas veins in normal limbs are rather straight. To validate the observed curvature, we simulated the deformation of an overturned fold using 2DMove^{TM} (Midland Valley Exploration Ltd.) (Fig. 9.5a, b). Initial starting point is a competent single-layer, containing equally-spaced bedding-normal veins embedded in an incompetent matrix. Forward modelling is applied in which the initial layer is folded into a fold geometry that reflects the deformation observed in the study area. In the fold the line length is kept constant (fold class 1B, Ramsay and Huber, 1987). In 2D Move the module *flexural-slip unfold* has been used, which allows having simple shear in the sandstone during folding. Only a weak vein deformation is observed in the normal dipping layers due to minor rotation of the limb. In overturned limbs, the result of the forward modelling (Fig. 9.5c) shows strongly-curved veins with upper vein tips sheared towards the next anticline and the bottom vein tips sheared towards the syncline. Conform theoretical analysis of folding (Ramsay and Huber, 1987) maximum deformation occurs in the middle part of the limbs whereas deformation is absent in the hinge zones. This model corresponds well to the vein geometries observed in the North Eifel. In a second example, an upright fold geometry has been modelled (Fig. 9.5d). Results show that veins in NW- and SE-dipping limbs suffer from less deformation than in the case of the overturned fold.

The scale and simplicity of these examples are strongly exaggerated with respect to natural examples. Natural folds are more complex and flexural flow within a layer depends, amongst other factors, on the isotropy of internal fabric within the competent layer, presence of surrounding other competent layers and anisotropy of the matrix. Only a competent layer in a highly anisotropic medium may approximate the observed high amount of flexural flow within the layer (Hudleston and Lan, 1993; Torremans et al. 2014; Treagus and Fletcher, 2009). However, for simplification, because the shape and orientation of the vein deformation style corroborates the observations it is concluded that in the competent beds, original planar veins were deformed during flexural-flow folding. The normal fold limbs experienced less simple shear than the overturned limbs which have undergone more rotation and stress reorientation (cf. Jackson, 1991).

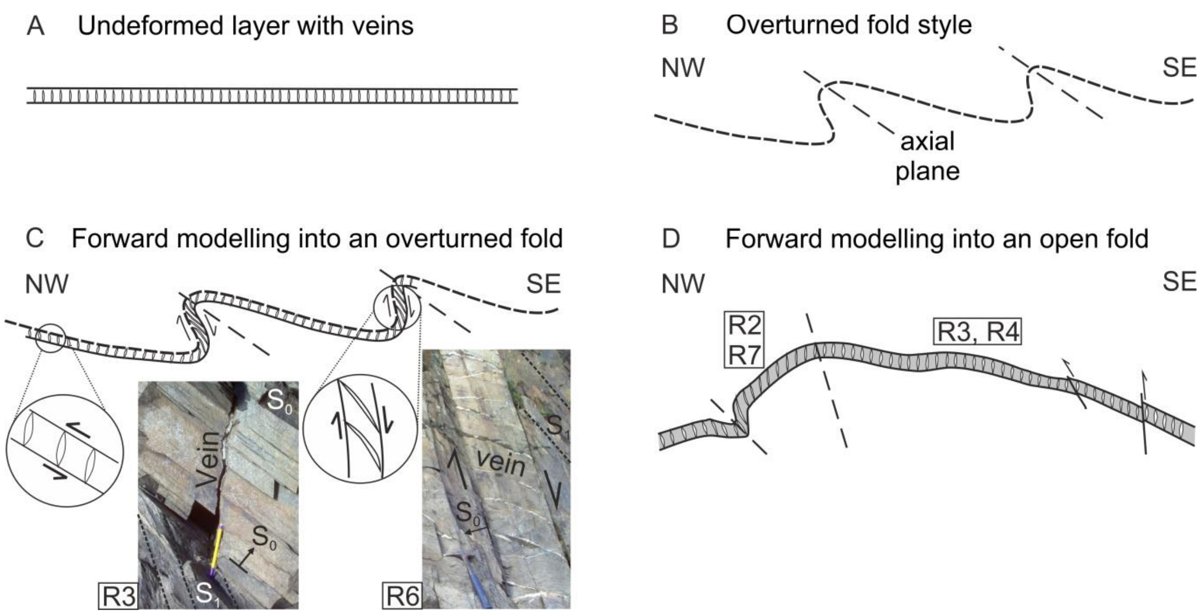

Figure 9.5: *Folding simulation using 2D Move (© Midland Valley).* ***a****) Horizontal sandstone bed with stratabound bedding-normal veins as starting point.* ***b****) Simplification of observed overturned folds at the Rursee.* ***c****) Forward model using the flexural-slip unfold module in 2D Move showing strongly curved veins in the overturned limbs and minor deformed veins in the normal limbs. Field pictures are used as comparison. Model scale exaggerated.* ***d****) Forward modelling into an open fold observed at the Rursee.* S_0*: bedding;* S_1*: cleavage.*

9.5.2 Consistent vein orientation throughout the HASB

In the Ardenne-Eifel Basin bedding-normal veins developed in Lower Devonian sandstones due to hydraulic fracturing from overpressured fluids present during a late burial stage (Hilgers et al., 2006, Kenis et al., 2002, Van Noten et al., 2011). Veins formed at high angle to bedding and vein infill often contains a fibrous fabric in which crack-seal microstructures exemplify the opening direction. The orientation of the unfolded veins can thus be used to detect the extensional stress state of the Ardenne-Eifel Basin at the time of fracturing. To derive principal stress axes of the regional stress tensor, the open source Win-Tensor program (version 5.8.6; Delvaux and Sperner, 2003) is used for each studied region but also other software such as T-Tecto (Žalohar & Vrabec, 2007) could be used. The results of the individual paleostress analyses are illustrated as small insets in Figure 9.3. We merged the unfolded veins of R1 to R7 (paleostress result shown on R7) and U1 to U5 (paleostress result shown on U5) to have an idea on consistent vein orientation in the Rursee and Urftsee, respectively.

The quartz veins formed in a consistent anisotropic Andersonian stress field with a vertical σ_1, corresponding to the overburden stress σ_V, and two well-defined horizontal principal stresses with $\sigma_2 > \sigma_3$, reflecting an extensional triaxial stress state during bedding-normal veining. In this stress state veins open parallel to σ_3. From the Rursee to Bertrix, over a distance of 120 kilometer, the Ardenne-Eifel Basin's stress state was consistent in orientation. Veins opened in an WNW-ESE direction in the North Eifel ($\sigma_{3,\ \mathrm{Rursee}}$=278°, $\sigma_{3,\ \mathrm{Urfstee}}$ =283°), in a NW-SE direction in the central part of the HASB ($\sigma_{3,\ \mathrm{Bütg.}}$= 303°, $\sigma_{3,\ \mathrm{Houff.}}$ = 298°, $\sigma_{3,\ \mathrm{Bast.}}$= 303°) and in a NNW-SSE at Bertrix ($\sigma_{3,\ \mathrm{Bertrix}}$ = 328°). The clockwise change in opening direction from WNW-ESE (Rursee) to NNW-SSE (Bertrix) results from oroclinal bending of the slate belt during the main Variscan contraction. This change in orientation corroborates with the difference in fold styles from the North Eifel (tight folds, NW verging) to the central HASB (open folds, NW verging) to southeastern part of the HASB (Bertrix, open folds, N verging).

9.6 Concluding remarks

In this chapter an unfolding exercise is presented in which bedding-normal quartz veins placed in folded, competent beds are restored or 'unfolded' into their original depositional position. Following standard stereonet procedures, a two-stage rotation methodology is applied in which, first, the tilt of the local fold hinge line and, second, the bedding dip is removed. 16 outcrops in the entire High-Ardenne slate belt were carefully selected to present a real unfolding exercise on the scale of a sedimentary basin. The results demonstrate that the orientation of unfolded the veins can be used to deduce a NW-SE opening direction of the Ardenne-Eifel Basin during a late burial stage. The results of this chapter can be reproduced in Structural Geology (practical) classes to investigate the usefulness in rotating a structural dataset.

Note that the unfolding methodology is only valid if folding in the main deformation phase is understood. In the single-deformed Ardenne-Eifel area folds formed by material rotation around the fold hinge line and later tilting did occur to lift up the beds and fold hinges. However, if multiple deformation phases have deformed a study area, one should be cautious in applying the two-stage methodology as it may be too straightforward.

9.7 Acknowledgements

We thank Dominique Similox-Tohon for his help with 2DMove™ (Midland Valley). The authors acknowledge the use of the Move Software Suite granted by Midland Valley's Academic Software Initiative. This research is partially financially supported by Research Grant OT/11/038 of the Onderzoeksfonds KU Leuven. The Elsevier team is thanked for proofreading.

9.8 Data availability

The dataset presented in this chapter is a shortened version of the full dataset provided in Van Noten (2011). The full georeferenced dataset (available in a Google Earth kmz file) can be requested by contacting the authors. This dataset includes vein, bedding, cleavage, intersection lineations and fold axes orientations gathered from outcrops along the Rursee and Urftsee lakes in the North Eifel.

9.9 References

Asselberghs, E., 1946. L'Eodévonien de l'Ardenne et des régions voisines. Mémoires de l'Institut géologique de l'Université de Louvain, 14, pp. 598.

Delvaux, D., Sperner, B., 2003. Stress tensor inversion from fault kinematic indicators and focal mechanism data: the TENSOR program. In: Nieuwland, D. (Ed.), New Insights Into Structural Interpretation and Modelling. Geological Society, London, Special Publications 212, pp. 75–100.

Derez, T., Pennock, G., Drury, M., Sintubin, M., 2016. Three sets of crystallographic sub-planar structures in quartz formed by tectonic deformation. Earth and Planetary Science Letters 442, 157-161.

Engelder, T. & Peacock, D.C.P. 2001. Joint development normal to regional compression during flexural-flow folding: the Lilstock buttress anticline, Somerset, England. *Journal of Structural Geology*, 23, 259-277.

Grohmann, C.H. and Campanha, G.A.C., 2010. OpenStereo: open source, cross-platform software for structural geology analysis. Presented at the AGU 2010 Fall Meeting, San Francisco, CA.

Hilgers, C., Bücker, C. & Urai, J.L. 2006. Fossil overpressures compartments? A case study from the Eifel area and some general aspects. In: Phillipp, S., Leiss, B., Vollbrecht, A., Tanner, D. & Gudmundsson, A. (eds) Symposium 'Tektonik, Struktur- und Kristallingeologie'. Universitätsdrucke,Göttingen, 87–89.

Hudleston, P.J., Lan, L., 1993. Information from fold shapes. Journal of Structural Geology 15, 153–264.

Jackson, R.R. 1991. Vein arrays and their relationship to transpression during fold development in the Culm Basin, central south-west England. *Proceedings of the Ussher Society* **7**, 356-362.

Kenis, I. 2004. Brittle-Ductile Deformation Behaviour in the Middle Crust as Exemplified by Mullions (Former "Boudins") in the High-Ardenne Slate Belt, Belgium. Aardkundige mededelingen 14, Leuven University Press.

Kenis, I., Sintubin, M., Muchez, Ph. & Burke, E.A.J. 2002. The "boudinage" question in the High-Ardenne Slate Belt (Belgium): a combined structural and fluid-inclusion approach. Tectonophysics 348, 93-110.

Kenis, I. and Sintubin, M. 2007. About boudins and mullions in the Ardenne-Eifel area (Belgium, Germany). Geologica Belgica 10, 79-91.

Lisle, R.J. and Leyshon. P.R., 2004. Stereographic Projection Techniques for Geologists and Civil Engineers. Second edition. Cambridge University Press, 112pp.

Lohest, M., Stainier, X. and Fourmarier, P., 1908. Compte rendu de la session extraordinaire de la Société géologique de Belgique, tenue à Eupen et Bastogne les 29, 30 et 31 août et le 1,2 et 3 septembre 1908. Annales de la Société géologique de Belgique, 36, 275-282.

Oncken, O., von Winterfeld, C.H. & Dittmar, U. 1999. Accretion of a rifted passive margin: The Late Paleozoic Rhenohercynian fold and thrust belt (Middle European Variscides). Tectonics 18, 75-91.

Parlangeau, C., Lacombe, O., Schueller, S., Daniel, J.-M., 2018. Inversion of calcite twin data for paleostress orientations and magnitudes: A new technique tested and calibrated on numerically-generated and natural data. Tectonophysics 722, 462-485.

Ramsay, J.G., Huber, M.I., 1987. The techniques of modern structural geology. Volume 2: folds and fractures. Academic Press, London.Tanner, G.P.W. 1989. The flexural-slip mechanism. Journal of Structural Geology 11, 635-655.

Torremans, K., Muchez, Ph., Sintubin, M. 2014. Mechanisms of flexural flow folding of competent single-layers as evidenced by folded fibrous dolomite veins. Journal of Structural Geology, 69, 75-90.

Treagus, S.H., Fletcher, R.C., 2009. Controls of folding on different scales in multilayered rocks. Journal of Structural Geology 31, 1340–1349.

Triantafyllou, A., Watlet, A., Bastin, C., 2017. Geolokit: An interactive tool for visualising and exploring geoscientific data in Google Earth. International Journal of Applied Earth Observation and Geoinformation 62, 39-46. http://geolokit.org/. (Last accessed 17 April 2018.)

Twiss, R.J. and Moores, E.M. 1992. Structural Geology. W.H. Freeman and Company, New York.

Van Noten, K., 2011. Stress-state evolution of the brittle upper crust during early tectonic Variscan inversion as defined by successive quartz vein-types in the High-Ardenne slate belt, Germany. Aardkundige mededelingen 28, 241p, Leuven University Press.

Van Noten, K., Hilgers, C., Urai, J.L., Sintubin, M., 2008. Late burial to early tectonic quartz veins in the periphery of the High-Ardenne slate belt (Rursee, North Eifel, Germany). Geologica Belgica 11, 179-198.

Van Noten, K., Berwouts, I., Muchez, Ph. & Sintubin, M. 2009. Evidence of pressure fluctuations recorded in crack-seal veins in low-grade metamorphic siliciclastic metasediments, Late Palaeozoic Rhenohercynian fold-and-thrust belt (Germany). Journal of Geochemical Exploration 101, 106.

Van Noten, K., Sintubin, M., 2010. Linear to non-linear relationship between vein spacing and layer thickness in centimetre- to decimetre-scale siliciclastic multilayers from the High-Ardenne slate belt (Belgium, Germany). Journal of Structural Geology 32, 377-391.

Van Noten, K., Muchez, P., Sintubin, M., 2011. Stress-state evolution of the brittle upper crust during compressional tectonic inversion as defined by successive quartz vein types (High-Ardenne slate belt, Germany). Journal of the Geological Society 168, 407-422.

Van Noten, K., Van Baelen, H., Sintubin, M., 2012. The complexity of 3D stress-state changes during compressional tectonic inversion at the onset of orogeny, in: Healy, D., Butler, R.W.H., Shipton, Z.K., Sibson, R.H. (Eds.), Faulting, Fracturing, and Igneous Intrusion in the Earth's crust. Geological Society, London, Special Publications 367, pp. 51-69.

Vergés, J., Burbank, D.W., Meigs, A. 1996. Unfolding: An inverse approach to fold kinematics. Geology, 24, 2, 175–178.

Žalohar, J., Vrabec, M. 2007. Paleostress analysis of heterogeneous fault-slip data: The Gauss method, J. Struct. Geol., 29, 1798–1810.